

Title	Structural Analysis of Molten Na ₂ BeF ₄ and NaBeF ₃ by X-ray Diffraction(Materials, Metallurgy, Weldability)
Author(s)	Iwamoto, Nobuya; Umesaki, Norimasa; Ohno, Hideo et al.
Citation	Transactions of JWRI. 1980, 9(2), p. 181-187
Version Type	VoR
URL	https://doi.org/10.18910/12021
rights	
Note	

Osaka University Knowledge Archive : OUKA

<https://ir.library.osaka-u.ac.jp/>

Osaka University

Structural Analysis of Molten Na_2BeF_4 and NaBeF_3 by X-ray Diffraction†

Nobuya IWAMOTO*, Norimasa UMESAKI**, Hideo OHNO*** and Kazuo FURUKAWA***

Abstract

The structures of molten Na_2BeF_4 ($650 \pm 10^\circ\text{C}$) and NaBeF_3 ($470 \pm 5^\circ\text{C}$) have been investigated by X-ray diffraction structural analysis. It is shown that BeF_4 tetrahedra existing in the crystalline state persist as the fundamental structural unit in the molten state. Molten Na_2BeF_4 contains mainly monomeric BeF_4^{2-} with four unshared F^- corners. A configuration for two Na^+ cations around a BeF_4 tetrahedron is suggested for molten Na_2BeF_4 . In molten NaBeF_3 , dimeric $\text{Be}_2\text{F}_7^{3-}$ with one shared F^- corner common to two BeF_4 tetrahedra appears. By comparison of the observed radial distribution functions $D(r)$ of molten NaBeF_3 and CaSiO_3 , it is concluded that both the chemicals have essentially the same structure.

KEY WORDS: (Structural Analysis) (Molten Na_2BeF_4) (Molten NaBeF_3) (X-ray Diffraction)

1. Introduction

The physical properties, such as self-diffusion¹⁾⁻³⁾, electrical conductance⁴⁾ and viscosity⁵⁾, etc., of molten alkali fluoroberyllates, XF ($\text{X} : \text{Li}, \text{Na}$ and K) - BeF_2 system, are greatly different from those of molten alkali halides due to the network character of beryllium fluoride. Moreover, it is known that a corresponding-state principle⁶⁾ is set up between the following pairs, (1) $\text{LiF} - \text{BeF}_2$ and $\text{MgO} - \text{SiO}_2$, (2) $\text{NaF} - \text{BeF}_2$ and $\text{CaO} - \text{SiO}_2$ and (3) $\text{KF} - \text{BeF}_2$ and $\text{BaO} - \text{SiO}_2$, in their intermediate composition regions under a reduced absolute temperature scale, and the physical properties, such as phase diagram, ionic packing density, self-diffusion coefficient, viscosity coefficient and equivalent conductivity in these pairs are in excellent agreement. We have measured the self-diffusion coefficients of lithium³⁾ and fluorine¹⁾²⁾ in molten Li_2BeF_4 and LiBeF_3 , respectively, and have shown the exchange mechanism of F^- between neighbouring beryllate units with the rotation of beryllate anions and the strong similarity between these molten alkali fluoroberyllates and molten silicates. However, further understanding of the structures of these molten alkali fluoroberyllates is essential for elucidating the mechanism of their physical properties. Up to data only a structural investigation of molten $\text{LiF} - \text{BeF}_2$ system using the X-ray diffraction method has been carried out by Vaslow and Narten⁷⁾.

They indicated only that Be^{2+} is tetrahedrally surrounded by four F^- in the melts.

In this paper, we report an X-ray diffraction structural analysis of molten Na_2BeF_4 and NaBeF_3 , and discuss the depolymerization mechanism of the network structure on the addition of sodium fluoride, and also show a structural similarity between molten NaBeF_3 and CaSiO_3 ⁸⁾ by comparison of the observed radial distribution functions $D(r)$ of these melts.

2. Experimental

Prior to the X-ray diffraction experiment, the samples were prepared as follows. The weighed amounts of analytical reagent grade NaF (prepared by Merck Co.) and BeF_2 (Rare Metallic Co.) were thoroughly mixed in a dry glove box and melted in a Pt crucible under a He atmosphere. After melting for about an hour, the samples were cooled and crushed.

The prepared samples were placed on a flat Pt tray ($35 \times 25 \times 3$ mm) and heated in a small electric furnace made of Pt wire. The sample-heater assembly was enclosed under a He atmosphere by putting it in an air-tight chamber with a window of Al foil of thickness $10 \mu\text{m}$ to allow passage of the X-ray beam. The temperature was

† Received on September 20, 1980

* Professor

** Research Associate

*** Molten Material Laboratory, Division of Nuclear Fuel Research, Japan Atomic Energy Research Institute

Transactions of JWRI is published by Welding Research Institute of Osaka University, Suita, Osaka, Japan

controlled to within a maximum error of 10 °C throughout the measurement.

The X-ray diffraction experiment was carried out with the use of a $\theta - \theta$ diffractometer with parafocusing reflexion geometry and Mo $K\alpha$ ($\lambda = 0.7107 \text{ \AA}$) monochromatized by a curved graphite monochromator mounted in the path of the diffracted beam. Slit systems of $1/2^\circ - 1/2^\circ$ and $1^\circ - 1^\circ$ were employed in the low ($3^\circ \leq \theta \leq 10^\circ$) and high ($8^\circ \leq \theta \leq 50^\circ$) scattering angles, respectively, where θ is the scattering angles. The X-ray scattering intensities were measured at 0.5° interval over the whole scattering angle range by way of the step-scanning technique. Several runs were made in order to accumulate 20000 counts per datum point in the low scattering angles and 34000 ~ 40000 in the high scattering angles.

The observed X-ray intensities were corrected for the background, polarization and Compton scattering, and then were scaled by means of the Krong-Moe-Norman method to the theoretical intensities arising from independent atoms contained in the stoichiometric unit. The radial distribution function $D(r)$, the correlation function $G(r)$, and the reduced intensity function $S \cdot i(S)$ are given as:

$$D(r) = 4\pi r^2 \rho_o \left[\sum_{i=1}^m \bar{K}_i + \sum_{i=1}^m (\bar{K}_i)^2 \frac{2r}{\pi} \int_0^{S_{\max}} S \cdot i(S) \sin(Sr) dS \right] \quad (1)$$

$$G(r) = 1 + \left[\sum_{i=1}^m (\bar{K}_i)^2 / \sum_{i=1}^m \bar{K}_i \pi^2 \rho_o r \right] \int_0^{S_{\max}} S \cdot i(S) \sin(Sr) dS \quad (2)$$

$$S \cdot i(S) = S \left[I_{\text{eu}}^{\text{coh}}(S) / \sum_{i=1}^m f_i(S)^2 - 1 \right] \quad (3)$$

where m is the number of atoms contained in the stoichiometric unit, \bar{K}_i the effective electron number of atom i , ρ_o the mean electron density, $f_i(S)$ the independent atomic scattering factor of atom i , $I_{\text{eu}}^{\text{coh}}(S)$ the total coherent scattering intensity and S_{\max} the maximum value of S ($= 4\pi \sin\theta/\lambda$) reached in the diffraction experiment. The constants used in the calculation of Eqs. (1), (2) and (3) are given in Table 1.

3. Results and Discussion

Fig. 1 shows the observed reduced intensity function $S \cdot i(S)$ of molten Na_2BeF_4 ($650 \pm 10^\circ\text{C}$) and NaBeF_3 ($470 \pm 5^\circ\text{C}$). The radial distribution functions $D(r)$, the functions $D(r)/r$ and the correlation functions $G(r)$ are shown in Figs. 2 and 3. As shown in Figs. 2 and 3, these curves indicate peaks at $1.60 \sim 1.65 \text{ \AA}$, $2.22 \sim 2.35 \text{ \AA}$, $2.26 \sim 2.66 \text{ \AA}$ and so on. Table 2 shows the distances and coordination numbers of the ionic pairs in molten Na_2BeF_4 and

Table 1 Constants used in the calculations of Eqs. (1), (2) and (3)

	Na_2BeF_4	NaBeF_3
temperature ($^\circ\text{C}$)	650 ± 10	470 ± 5
density (g/cm^3) ¹⁾	2.093	2.133
molar weight	130.997	88.991
N_{Na}	2	1
N_{Be}	1	1
N_{F}	4	3
effective electron number		
\bar{K}_{Na}	11.84	11.98
\bar{K}_{Be}	3.73	3.77
\bar{K}_{F}	8.65	8.75
S_{\max} (\AA^{-1})	13.5	13.0

NaBeF_3 derived from the functions $D(r)/r$ by assuming a Gaussian distribution¹⁰⁾. In the known crystalline forms of some alkali fluoroberyllates such as Na_2BeF_4 ¹¹⁾ and Li_2BeF_4 ¹²⁾, each Be^{2+} is tetrahedrally surrounded by four F^- with Be-F distance of $1.54 \sim 1.56 \text{ \AA}$ and F-F distance of $2.50 \sim 2.56 \text{ \AA}$. Therefore, the first peaks at $1.60 \sim 1.65 \text{ \AA}$ and the third peaks at $2.60 \sim 2.65 \text{ \AA}$ of the observed curves are due to Be-F and F-F pairs in the BeF_4 tetrahedra. In addition, the observed coordination number of the nearest neighbouring F^- around Be^{2+} , $n_{\text{Be}/\text{F}}$, is about $3.4 \sim 4.0$. These results indicate that BeF_4 tetrahedra existing in the crystalline state persist as the fundamental structural unit in the molten state, and the mean distances between the ions in a BeF_4 tetrahedron become slightly longer in the melt than in the solid. The second peaks at $2.22 \sim 2.35 \text{ \AA}$ are due to the nearest neighbouring Na-F, between which ions the distance is nearly the sum of the ionic radii¹³⁾ of Na^+ (0.95 \AA) and F^- (1.36 \AA).

Molten Na_2BeF_4

In molten Na_2BeF_4 , the observed coordination number of F-F pairs in BeF_4 tetrahedra, $n_{\text{F}/\text{F}}$, is 3.0. This suggests that BeF_4 tetrahedra exist mainly in the isolated form with four unshared F^- corners, monomeric BeF_4^{2-} , in molten Na_2BeF_4 . Quist et al¹⁴⁾ showed, using Raman spectroscopy measurement, that monomeric BeF_4^{2-} was the only beryllium-containing species in molten Na_2BeF_4 and Li_2BeF_4 . A similar result was pointed out from e.m.f. measurement of molten LiF- BeF_2 system by Holm and Kleppa¹⁵⁾. They reported that, up to $x_{\text{BeF}_2} =$

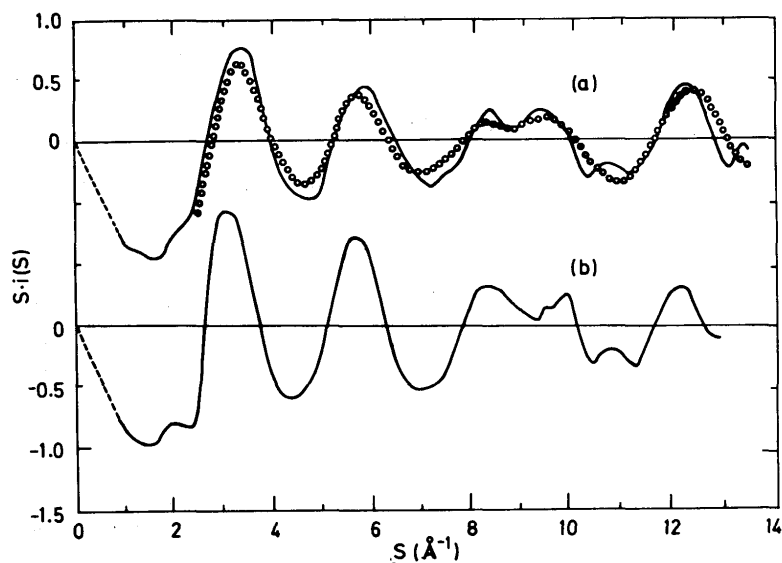


Fig. 1 Observed (full line) and calculated (open circle) reduced intensity functions $S_i(S)$ of (a) molten Na_2BeF_4 ($650 \pm 10^\circ\text{C}$) and (b) molten NaBeF_3 ($470 \pm 5^\circ\text{C}$).

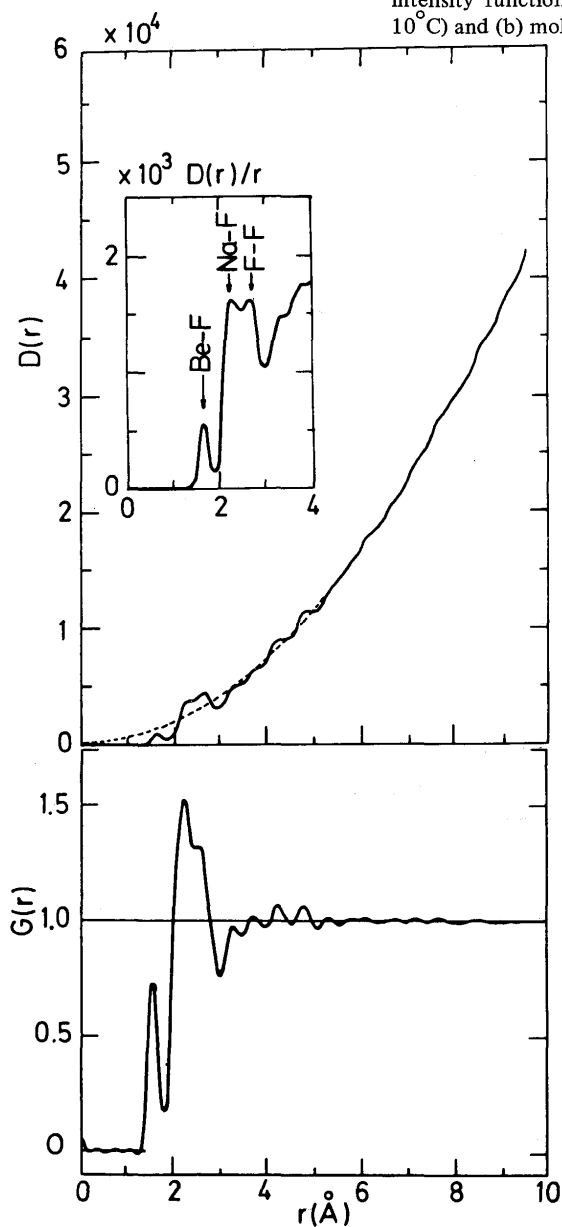


Fig. 2 Radial Distribution function $D(r)$, function $D(r)/r$ and correlation function $G(r)$ of molten Na_2BeF_4 ($650 \pm 10^\circ\text{C}$).

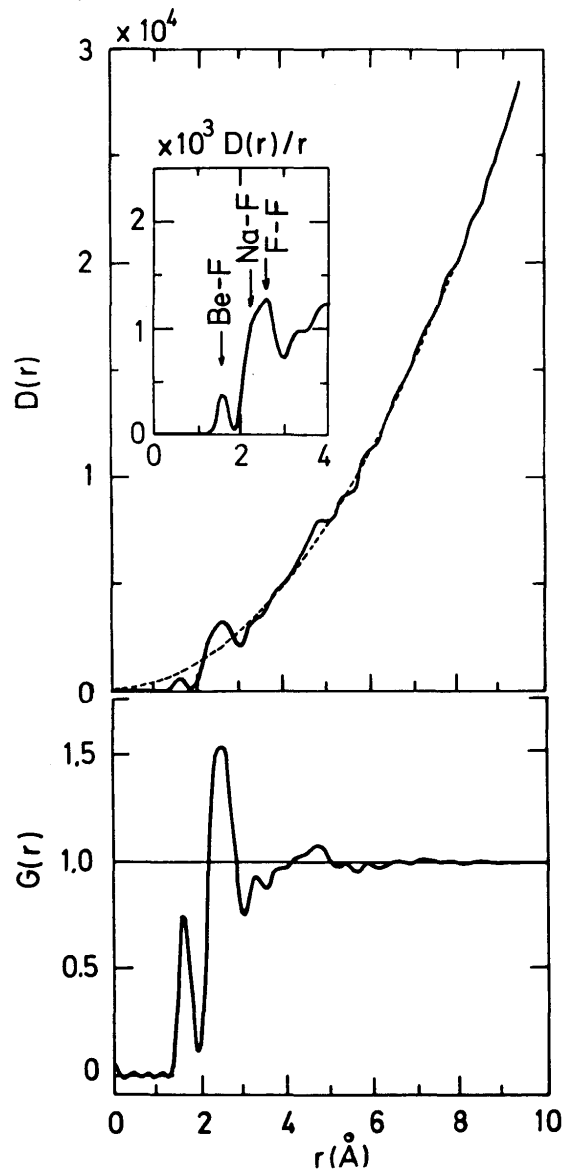


Fig. 3 Radial Distribution function $D(r)$, function $D(r)/r$ and correlation function $G(r)$ of molten NaBeF_3 ($470 \pm 5^\circ\text{C}$).

Table 2 The observed distances and coordination numbers of the ionic pairs in molten Na_2BeF_4 and NaBeF_3 .

		liquid		crystal	sum of ionic radii
		Na_2BeF_4 (650±10°C)	NaBeF_3 (470±5°C)	Na_2BeF_4 Deganello 1973	
Be-F	$r_{\text{Be-F}}$ (Å)	1.65	1.60	1.54~1.56	1.67
	$n_{\text{Be/F}}$	4.0	3.4	2.27~2.54	
Na-F	$r_{\text{Na-F}}$ (Å)	2.22	2.35	2.27~2.54	2.31
	$n_{\text{Na/F}}$	2.8	1.8		
F-F	$r_{\text{F-F}}$ (Å)	2.65	2.60	2.50~2.56	2.72
	$n_{\text{F/F}}$	3.0	3.5		

0.33 corresponding to the composition of Li_2BeF_4 , the partial molar excess entropy of beryllium fluoride was positive and changed little with composition due to complete depolymerization of the network structure of beryllium fluoride, that is, the formation of monomeric BeF_4^{2-} . Therefore, it is considered that the significant feature of molten Na_2BeF_4 consist of Na^+ cations and monomeric BeF_4^{2-} anions bonding by Coulombic forces. Most of the Na^+ might occupy the several stable positions around monomeric BeF_4^{2-} for some time and then migrate to other stable positions through voids in the melt. In order to advance understanding of the transport properties of molten Na_2BeF_4 , the stable positions occupies by Na^+ around a BeF_4 tetrahedron would have to be clarified. The following three typical configuration can be supposed: a Na^+ occupies (a) the corner-site position, (b) the edge-site position and/or (c) the face-site position around a BeF_4 tetrahedron, as shown in Fig. 4. Structural models of various combinations of these typical configurations were constructed taking into consideration of the stoichiometric unit, and compared with the observed S-i(S) curve using the Debye scattering Eq. (4)¹⁶⁾ as:

$$S \cdot i(S) \left\{ \sum_{i=1}^m f_i(S)^2 \right\} = \sum_{i=1}^m \sum_j f_i(S) f_j(S) \exp(-b_{ij} S^2) \sin(Sr_{ij}) / r_{ij}, \quad (4)$$

where $f_i(S)$ and $f_j(S)$ are the independent atomic scattering factors or atoms i and j ; r_{ij} the distance between ions i and j and b_{ij} the temperature factor that is half of the mean square variation in r_{ij} . The lower limit of S in the

S-i(S) curve depends on the size of the structural model; since it is about the maximum intraionic distance in the structural model, we examined the range $2.0 \text{ \AA}^{-1} \leq S \leq 13.5 \text{ \AA}^{-1}$. Fig. 5 shows a comparison of the calculated S-i(S) curves of three typical configurations ((a), (b) and (c) in Fig. 4) with the observed one. The most possible structure, showing the best fit for the observed S-i(S) curve as shown in Fig. 1, is made up of two Na^+ around a BeF_4 tetrahedron, that is, one of the two Na^+ occupies the corner-site position ((a) in Fig. 4) and the other occupies the edge-site position ((b) in Fig. 4). The constants used in the calculation were obtained by a least square variation of Eq. (4) against the observed S-i(S) curve, and are given in Table 2. The coordination number of the nearest neighbouring Na-F pair, $n_{\text{Na/F}}$, in this model is 3.0 which is almost equal to the observed one. From measurement of the spin-lattice relaxation time for molten Li_2BeF_4 , LiBeF_3 and NaBeF_3 by means of nuclear magnetic resonance, Matsuo and Suzuki¹⁷⁾ pointed out the possibility of the edge-site position of Na^+ around the BeF_4 tetrahedron.

A subsequent communication will be discussed a long-range arrangement of neighbouring Na_2BeF_4 units around a Na_2BeF_4 unit.

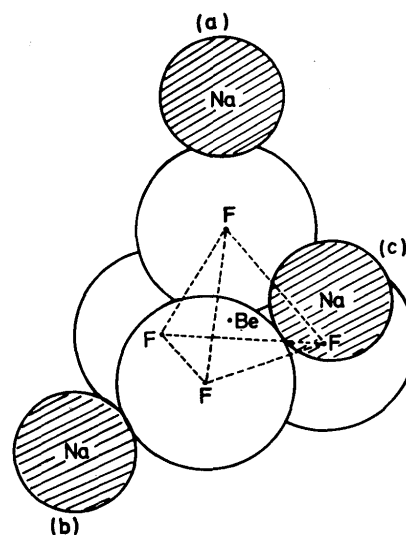


Fig. 4 Schematic illustration of typical configurations of Na^+ ions around a BeF_4 tetrahedron. (a) corner-site position; (b) edge-site position; (c) face-site position.

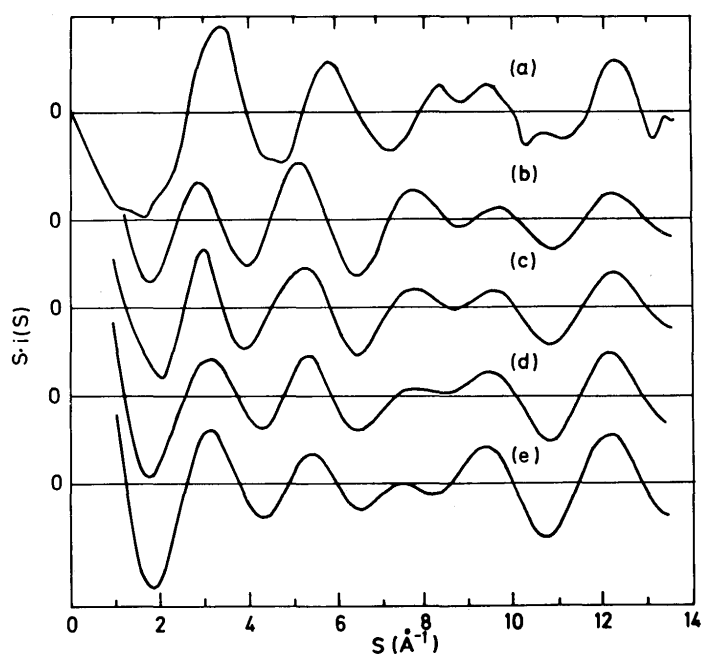


Fig. 5 Comparison of observed (molten Na₂BeF₄) and calculated $S \cdot i(S)$ curves. (a) observed; (b) a BeF₄ tetrahedron; (c) corner-site position; (d) edge-site position; (e) face-site position.

Table 3 Constants used in the calculation of the most possible structural model by Eq. (4). $N_{i/j}$, r_{ij} and $\langle \Delta r_{ij}^2 \rangle^{1/2}$ are the coordination numbers of j ions around any origin i ion, the distance and the associated root mean square displacement between ions i and j , respectively.

i	j	$N_{i/j}$	r_{i-j} (Å)	$\langle \Delta r_{i-j}^2 \rangle^{1/2}$ (Å)
Na	Na	2.0	—	—
Be	Be	1.0	—	—
F	F	4.0	—	—
Be	F	8.0	1.65	0.100
F	F	12.0	2.62	0.141
Na	Be	1.0	3.32	0.142
Na	Be	1.0	4.19	0.142
Na	F	3.0	2.22	0.110
Na	F	2.0	3.76	0.236
Na	F	3.0	4.64	0.285
Na	Na	2.0	5.37	0.437

Molten NaBeF₃

Up to the composition range of Na₂BeF₄, the mixtures rich in sodium fluoride will chiefly contain Na⁺ cations, F⁻ and monomeric BeF₄²⁻ anions. As the region rich in

beryllium fluoride attained, the polymerization process proceeds and molten pure beryllium fluoride forms three-dimensional network structure of BeF₄ tetrahedra. NaBeF₃ is intermediate between these composition range. From viscosity⁵⁾ and thermodynamics data¹⁵⁾, we can estimate that a mixture with the composition of NaBeF₃ contains a high percentage of some polymeric anions with small size.

In molten NaBeF₃, the observed coordination number $n_{F/F}$ was 3.5. This value is close to the $n_{F/F}$ of the following three dimeric anions: (1) the corner sharing Be₂F₇³⁻ ($n_{F/F} = 3.5$), (2) the edge sharing Be₂F₆²⁻ ($n_{F/F} = 3.8$) and (3) the face sharing Be₂F₅⁻ ($n_{F/F} = 3.6$). However, the existence of Be₂F₆²⁻ and Be₂F₅⁻ is not supported due to the following reasons: (1) because of the remarkable decrease in the distance of the two Be²⁺ within Be₂F₆²⁻ and Be₂F₅⁻ compared to within Be₂F₇³⁻, the repulsive forces between these two Be₂ within Be₂F₆²⁻ and Be₂F₅⁻ increase, and these two dimeric anions would be accordingly unstable. (2) only corner sharing anions are found in analogous silicate systems, and (3) the existence of Be₂F₃⁻ in molten Na₂LiBe₂F₇ was pointed out from measurement using Raman spectroscopy¹⁸⁾. Therefore, the main polymeric anion in molten NaBeF₃ would be dimeric Be₂F₇³⁻. In addition, the observed coordination number $n_{Na/F}$ was 1.8. Na⁺ cations are presumably placed in contact with the two unshared F⁻ corners of the two Be₂F₇³⁻.

As was noted above in the introduction, a molten $\text{NaF}^{\cdot}\text{BeF}_2$ system would have essentially the same structure as a molten CaO-SiO_2 system by the corresponding-state principle⁶⁾. X-ray structural analysis of molten CaSiO_3 only was carried out Waseda and Toguri⁸⁾. We examined the similarity of this to the structure of molten NaBeF_3 (measured temperature: $T = 743$ K, m.p. temperature: $T_m = 645$ K, reduced absolute temperature scale: $T/T_m = 1.15$) and that of molten CaSiO_3 ($T = 1873$ K, $T_m = 1813$ K, $T/T_m = 1.03$). Fig. 6 shows a comparison of the observed $D(r)$ curves of these chemicals. The value peak positions of both $D(r)$ curves show good agreement. Therefore, by analogy with $\text{Be}_2\text{F}_7^{3-}$ in molten NaBeF_3 , $\text{Si}_2\text{O}_7^{6-}$ would also exist in molten CaSiO_3 . It is well known that there are two configurations, that is, the eclipsed ((a) in Fig. 7) and staggered ((b) in Fig. 7) forms for dimeric anions which consist of two tetrahedra sharing one common F^- corner. As shown in Fig. 6, the peak positions of the two forms in $\text{Be}_2\text{F}_7^{3-}$ and $\text{Si}_2\text{O}_7^{6-}$ qualitatively coincide with those of the observed $D(r)$

curves of molten NaBeF_3 and CaSiO_3 . This result leads to the conclusion that both the chemicals have essentially the same structure.

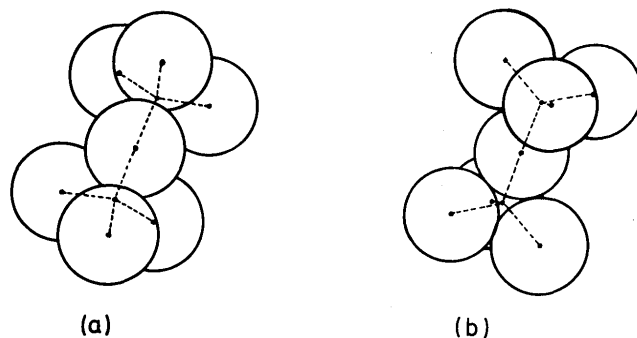


Fig. 7 Configurations of dimeric A_2X_7 ions. (a) eclipsed form; (b) staggered form.

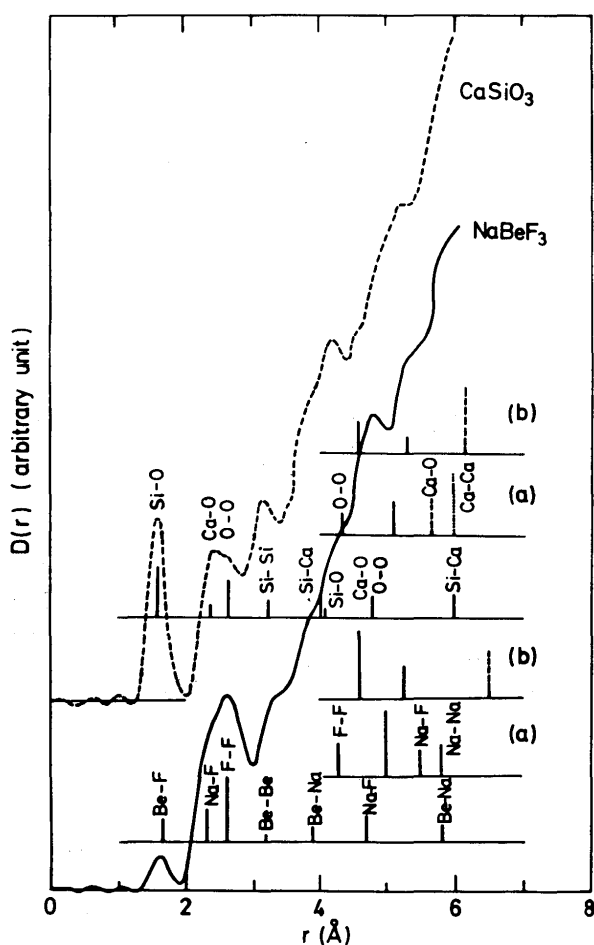


Fig. 6 Comparison of $D(r)$ curves of molten NaBeF_3 ($470 \pm 5^\circ\text{C}$, $T/T_m = 1.15$) and CaSiO_3 (1600°C , $T/T_m = 1.03$). T : experimental temperature; T_m : m.p. temperature. (a) eclipsed form. (b) staggered form.

4. Conclusion

From the results obtained, we can summarize as follow,

- (1) In molten Na_2BeF_4 and NaBeF_3 , BeF_4 tetrahedra exist as the fundamental structural unit. The mean distances of the ionic pairs in a BeF_4 tetrahedron become slightly longer in the melts than those found in the solid. The mean distances of the nearest neighbouring Na-F pair are close to the sum of the ionic radii of Na^+ and F^- .
- (2) Molten Na_2BeF_4 contains mainly monomeric BeF_4^{2-} with four unshared F^- corners. This result is supported by the results of Raman spectroscopy and e.m.f. measurements. Furthermore, two Na^+ are situated in the following configurations around a BeF_4 tetrahedron: one of the two Na^+ occupies the corner-site position and the other occupies the edge-site position.
- (3) Dimeric $\text{Be}_2\text{F}_7^{3-}$ with one shared F^- corner common to two BeF_4 tetrahedra appears in molten NaBeF_3 . From comparison of the observed $D(r)$ curves of molten NaBeF_3 and CaSiO_3 , both the chemicals have essentially the same structure.

Acknowledgements

The authors thank Mr. Y. Takagi (Research Laboratory of Engineering Materials, Tokyo Institute of Technology) for useful suggestions during this work.

References

- 1) T. Ohmichi, H. Ohno and K. Furukawa : J. Phys. Chem., 80 (1976), p. 1628.
- 2) H. Ohno, Y. Tsunawaki, N. Umesaki, K. Furukawa and N. Iwamoto : J. Chem. Res. (M), 1978, P. 2048.
- 3) N. Iwamoto, Y. Tsunawaki, N. Umesaki, H. Ohno and K. Furukawa : J. Chem. Soc. Faraday Trans. II, 75(1979), p.1277.
- 4) G. D. Robbins and J. Braunstein : MSR Program Seminar Prog. Rept., ORNL-458, 1970, p. 156-159.
- 5) S. Cantors, W. T. Ward and C. T. Moynihan : J. Chem. Phys., 50 (1969), p. 2874.
- 6) K. Furukawa and H. Ohno : Trans. Japan Inst. Met., 19 (1978)
- 7) F. Vaslow and A. H. Narten : J. Chem. Phys., 59 (1973), p. 4949.
- 8) Y. Waseda and J. M. Toguri : Met. Trans., 8B (1976), p. 563.
- 9) B. C. Blanke, K. W. Foster, L. V. Jones, K. C. Jordan, R. W. Joyner and E. L. Murphy : MLM-1079, 1958, p. 1-90.
- 10) C. A. Coupson and G. S. Roushbrooke : Phys. Rev., 56 (1939), p. 1216.
- 11) S. Deaganello : Acta Cryst., B29 (1973), p. 2593.
- 12) J. H. Burns and E. K. Gordon : Acta Cryst., 20 (1966), p. 135.
- 13) L. Pauling : Nature of The Chemical Bond, 3d ed. Ithaca, N.Y. : Cornello University Press, (1960).
- 14) A. S. Quist, J. B. Bates and G. E. Boyd : J. Phys. Chem., 76 (1972), p. 78.
- 15) J. L. Holm and J. O. Kleppa : Inorg. Chem., 8 (1969), p. 207.
- 16) H. A. Levy, M. D. Danford and A. H. Narten : ORNL Rept. No. ORNL-3960, p. 1-56.
- 17) Y. Matsuo and H. Suzuki : personal communication.
- 18) L. M. Toth, J. B. Bates and G. E. Boyd : J. Phys. Chem., 77 (1973), p. 216.